Letter

Mining public domain data to develop selective DYRK1A inhibitors

Scott H Henderson, Fiona Sorrell, James Bennett, Marcus T Hanley, Sean Robinson, Iva Hopkins Navratilova, Jonathan M Elkins, and Simon E Ward

ACS Med. Chem. Lett., **Just Accepted Manuscript** • DOI: 10.1021/acsmedchemlett.0c00279 • Publication Date (Web): 30 Jun 2020

Mining public domain data to develop selective DYRK1A inhibitors

Scott H. Henderson[†,*], Fiona Sorrell[#], James Bennett[§], Marcus T. Hanley[‡], Sean Robinson[ǁ], Iva Hopkins Navratilova[ǁ,≠], Jonathan M. Elkins[#,⊥], Simon E. Ward[‡,*].

[†]Sussex Drug Discovery Centre, University of Sussex, Brighton, BN1 9RH, U.K.

[#]Structural Genomics Consortium, University of Oxford, Old Road Campus Research Building, Oxford, OX3 7DQ, U.K.

[§]Target Discovery Institute, University of Oxford, Oxford, OX3 7FZ, UK.

[ǁ]Exscientia, The Schrödinger Building, Oxford Science Park, Oxford OX4 4GE, UK.

[≠]University of Dundee, Dow Street, Dundee, DD1 5EH, U.K.

[⊥]Structural Genomics Consortium, Universidade Estadual de Campinas, Cidade Universitária Zeferino Vaz, Av. Dr. André Tosello, 550, Barão Geraldo, Campinas, SP 13083-886, Brazil.

[‡]Medicines Discovery Institute, Cardiff University, CF10 3AT, U.K.

ABSTRACT: Kinases represent one of the most intensively pursued groups of targets in modern-day drug discovery. Often it is desirable to achieve selective inhibition of the kinase of interest over the remaining ~500 kinases in the human kinome. This is especially true when inhibitors are intended to be used to study the biology of the target of interest. We present a pipeline of open-source software that analyzes public domain data to repurpose compounds that have been used in previous kinase inhibitor development projects. We define the dual-specificity tyrosine-regulated kinase 1A (DYRK1A) as the kinase of interest, and by addition of a single methyl group to the chosen starting point we remove glycogen synthase kinase β (GSK3β) and cyclin-dependent kinase (CDK) inhibition. Thus, in an efficient manner we repurpose a GSK3β/CDK chemotype to deliver **8b**, a highly selective DYRK1A inhibitor.

KEYWORDS. *DYRK1A, polypharmacology, chemoinformatics, selectivity.*

Introduction

In recent years clinical successes have demonstrated the large potential of kinase inhibitors to become approved drugs.[1] However, achieving the desired selectivity profile remains a significant challenge. A number of general methods to gain selectivity have been documented, such as targeting the non-conserved, inactive DFG-out (Type II) conformation of the kinase,[2] allosteric-site directed (Type III) inhibition[3] or compounds that access a non-conserved pocket behind the gatekeeper residue (Type I$^{1/2}$).[4] Thus far, the majority of FDA-approved kinase inhibitors are found to bind in a conventional Type I, ATP competitive mode.

Kinase profiling data contains both on- and off-target data for compounds often from the same chemical class, derived from the same data source. Routine assessment of off-target activity facilitates the design of a desired selectivity profile, in order to minimize off-target-related side effects. With the availability of large kinase screening panels various large scale sets of homogenous screening data for many compounds against many kinases have been reported. These include significant kinase datasets from Anastassiadis *et al.*,[5] Davis *et al.*,[2] Metz *et al.*,[6] as well as the screening data derived from the Published Kinase Inhibitor Sets 1 and 2 (PKIS/PKIS2).[7,8,9] Many of these compound sets are comprised of molecules in the realms of drug-like space, originating from pharmaceutical industry drug discovery programs. These compounds and associated data provide opportunities for repurposing kinase inhibitors for targets of current interest.

The ChEMBL database[10] holds records for over 1.3 million compounds, with around 10 million compound bioactivity measurements derived from published structure-activity relationship studies and compound library screening studies. An effective data-mining strategy is essential to utilise this information. The Konstanz Information Miner (KNIME®) is an open source data analytics platform that can be used to mine ChEMBL using pre-made workflows.[11] ChEMBL KNIME® nodes and the NN-Activity Pairs workflow were developed by workers at ChEMBL-EBI to highlight the polypharmacology profiles of similar compounds within a cluster (nearest neighbours). Differences in the polypharmacology profiles of nearest neighbours can be interrogated to identify chemical transformations that lead to better selectivity. The principles of

the NN-Activity Pairs workflow is shown in Figure 1 (a schematic of the workflow is available in supplementary information Figure SI-1).

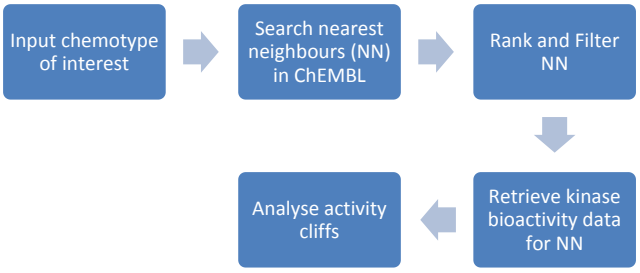

Figure 1. Principles of workflow used to mine kinase profiling data. The workflow was implemented in KNIME® using the 'NN Activity Pairs' workflow to mine ChEMBL.

In the case where the binding mode of the series is known, the position of the chemical transformation that has led to an improvement in selectivity can be valuable in the design of selective inhibitors. We illustrate the value of this approach in the context of a target of current interest, dual-specificity tyrosine-regulated kinase 1A (DYRK1A). We successfully remove two key off-targets by utilizing the KNIME® workflow.

DYRK1A is of interest for inhibitor development due to its purported roles in the development and progression of neurodegenerative disorders such as Alzheimer's Disease (AD),[12] Huntington's Disease (HD) and Parkinson's Disease (PD).[13,14,15,16] The DYRK1A gene is located on the Down's syndrome critical region of chromosome 21, consequently, individuals with Down's syndrome express elevated levels of DYRK1A protein.[17] Microduplication of the DYRK1A gene resulted in dysmorphic and intellectual features characteristic of a Down's syndrome phenotype, supporting the hypothesis that DYRK1A represents a novel target for the treatment of Down's syndrome.[18] Increased tau phosphorylation is observed in trisomy[19,20] and Down's syndrome is associated with early-onset AD, underscoring a genetic link between DYRK1A, AD and Down's syndrome.[21,22,23,24,25]

Several DYRK1A inhibitors have been developed and summarized in recent reviews.[12,26] Although many are reported as potent DYRK1A inhibitors, the majority of inhibitors have not had their kinome-wide selectivity profiles reported; those that have inhibit other members of the CMGC group[27] of kinases. Given the lack of reported DYRK1A inhibitors progressing into and beyond clinical trials, there remains a need to develop high quality chemical matter which can be used for detailed biological study.[28] Investigation of neurodevelopment or neurodegeneration requires a CNS penetrant inhibitor, capable of exerting an on-target effect *in vivo*. Two of the most advanced DYRK1A inhibitors so far published are L41[29] and EHT 5372,[30] which exhibit good potency and kinome-wide selectivity. However, both possess potent off-target activity at other CMGC kinases. L41 inhibits CLKs and GSK3β,[29] a kinase for which DYRK1A serves as a priming kinase, and which regulates many of the same signalling pathways as DYRK1A.[31] Another CMGC kinase family that is often inhibited by DYRK1A inhibitors is the cyclin-dependent kinases (CDKs).[32] Despite the availability of structural data, it has been difficult to gain DYRK1A selectivity against CLKs, GSK3β and the CDKs, while optimizing DYRK1A inhibitory activity.

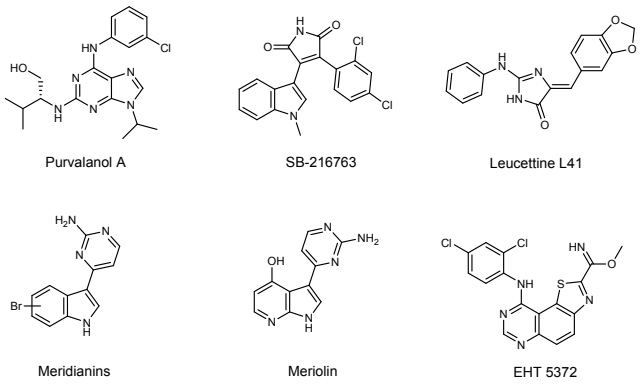

Figure 2. Known DYRK1A inhibitors that also inhibit CMGC kinases, including GSK3s and CDKs.

Results and Discussion

Data mining identified a pyrazolo[1,5-*b*]pyridazine starting point

Inspection of publicly available kinase profiling data led to the identification of a cluster of kinase inhibitors based on the pyrazolo[1,5-*b*]pyridazine core with the potential to become a novel and drug-like DYRK1A template.[7-9] The pyrazolo[1,5-*b*]pyridazines were attractive starting points in terms of drug-like properties, DYRK1A binding affinity and kinome-wide selectivity. However, the series originated from former GSK3β[33] and CDK inhibitor programs.[34] Selectively removing inhibition of these two kinases, while maintaining DYRK1A binding affinity and the overall kinome-wide selectivity profile, was envisaged as a way to afford a selective DYRK1A tool compound.

The NN-Activity Pairs KNIME® workflow was used to mine ChEMBL to highlight the polypharmacology profiles of nearest neighbours. Inspection of the Kinase Activity Profile histogram (supplementary information, Figure SI-2) for the pyrazolo[1,5-*b*]pyridazines revealed a number of matched-molecular pairs (MMPs) and chemical transformations that led to significant decreases in inhibitory activity against GSK3β and CDK2 (Figure 3).

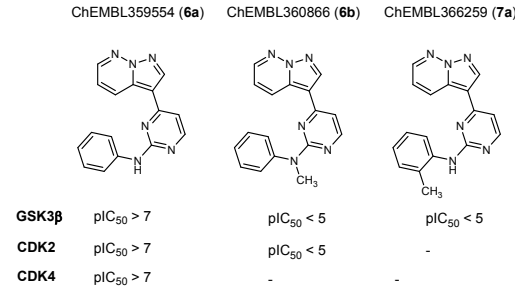

Figure 3. Activity cliffs identified rapidly from NN-Activity Pairs KNIME® workflow. Data from ChEMBL.[10]

Chemistry

An advantage of using publicly available profiling data as a starting point for inhibitor discovery is that information regarding synthetic routes has usually already been published. Following the published procedure,[33,34] the aminated pyridazine **2** was formed in excellent yield after reaction of pyridazine **1** with hydroxylamine-*O*-sulfonic acid (HOSA). Subsequent [3+2] cycloaddition between **2** and butyne-2-one afforded the pyrazolo[1,5-*b*]pyridazine **3** in average yield. DMF/DMA condensation furnished the corresponding enamine **4** in excellent yield. Conversion of **4** to the corresponding pyrimidine was slow under conventional heating at elevated temperatures, taking up to 48 hours for the formation of the desired product to occur (Scheme 1).

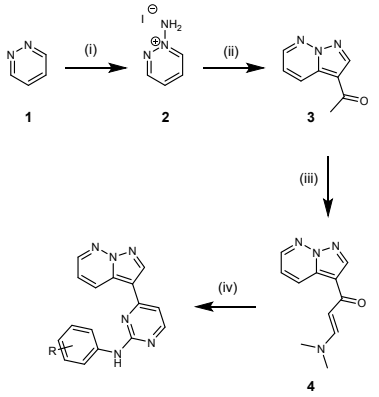

Scheme 1. *Reagents and conditions:* (i) hydroxylamine-*O*-sulfonic acid, $KHCO_3$, KI, H_2O, 70 °C, 1.5 h, 94%; (ii) butyne-2-one, KOH, CH_2Cl_2, rt, 16 h, 60%; (iii) DMF-DMA, 100 °C, 16 h, 91%; (iv) phenyl guanidines, 2-methoxyethanol, 110 °C, 16-48 h, 13-37%.

One disadvantage of the literature synthesis was that the preparation of each analogue required the respective phenyl guanidine to be synthesised first and in most cases the synthesis of the phenyl guanidine was low yielding. Phenyl guanidines were prepared using concentrated nitric acid and cyanamide from the corresponding aniline (Scheme 2).[33,34]

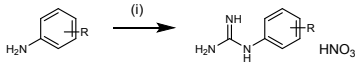

Scheme 2. *Reagents and conditions:* (i) cyanamide (50 wt.% in H_2O), HNO_3, EtOH, 100 °C, 16-48 h, 35-62%.

In an effort to improve the versatility of the synthesis, the chloropyrimidine intermediate **5** was prepared. Nucleophilic aromatic substitution with a range of nucleophiles was then possible. Scale-up of **5** was completed in high yield from **4** (Scheme 3).

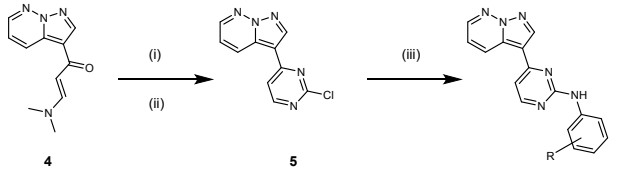

Scheme 3. *Reagents and conditions:* (i) urea, sodium, 140 °C, 10 min, 91%; (ii) phosphorus(V)oxychloride, 110 °C, 3 h, 92%; (iii) conditions A: anilines, 2-propanol, 150 °C, 2-16 h, 4-44%; conditions B: anilines, 2-propanol, 150 °C, 15-20 min, microwave, 43-60%.

Two approaches were taken to install the *N*-methyl substituent onto the aminopyrimidine. Nucleophilic aromatic substitution of **5** with *N*-methylbenzylamine afforded **6b** in 44% yield. Alternatively, *N*-methylation with sodium hydride and iodomethane was carried out on late-stage analogues, **8a** and **10a** to access **8b** and **10b** respectively (Scheme 4).

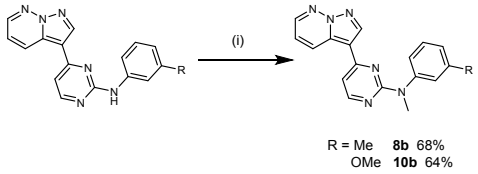

Scheme 4. *Reagents and conditions:* (i) sodium hydride, iodomethane, DMF, rt, 2 h.

Inhibitor Optimization

The MMPs with the most complete dataset were **6a** and **6b** (Figure 3). The data suggested that *N*-methylation of the aminopyrimidine N-*H* reduced the inhibitory activity at both GSK3β and CDK2 of the pyrazolo[1,5-*b*]pyridazine series by 2 log units. Pyrazolo[1,5-*b*]pyridazine analogues that were inactive against GSK3β and CDKs were of great interest as DYRK1A inhibitors. *N*-methylation was an attractive strategy to pursue for gaining selectivity as the number of hydrogen-bond donors in the series was reduced simultaneously, which could improve permeability and CNS penetration of the series.

To confirm that *N*-methylation afforded selectivity against the original series off-targets, GSK3β and CDK2, **6a** and **6b** were profiled in a radiometric kinase assay (^{33}PanQinase® Activity Assay) provided by Proqinase GMBH. The assay measured the kinase activity of DYRK1A, GSK3β and CDK2 in the presence and absence of inhibitors. Gratifyingly, the selectivity profile predicted in KNIME® was confirmed experimentally, with **6b** displaying selective inhibition of DYRK1A, whereas **6a** inhibited all three CMGC kinases.

Table 1: CMGC Selectivity of **6a** and **6b** at 1 μM

Compound	DYRK1A[a]	GSK3β[a]	CDK2[a]
6a	97	76	98
6b	79	13	33

[a]% inhibition in ^{33}PanQinase® Activity Assay (n=1)

Several pyrazolo[1,5-*b*]pyridazines were profiled against DYRK1A in a binding-displacement assay (Table 2). In general, analogues possessing *meta*-substituents on the aniline ring exhibited stronger binding affinity for DYRK1A. Both electron-donating (**8a** and **10a**) and electron-withdrawing (**11a**) substituents were well-tolerated in the *meta*-position. Analogues with *ortho* and *para* substituents on the aniline ring exhibited weaker DYRK1A binding affinity - **7a** and **9a** exhibited approximately 10 fold weaker binding affinity than *meta* analogues **8a** and **10a**, whilst **12a** displayed 20 fold weaker binding affinity for DYRK1A than *meta* analogue **11a**.

Table 2. DYRK1A Binding Affinity of Pyrazolo[1,5-*b*]pyridazines

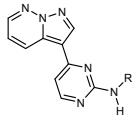

Compound	R	DYRK1A[a]
6a		38
7a		64
8a		7
9a		137
10a		12
11a		5
12a		103

[a]16-point IC_{50} (nM) in TR-FRET-based ligand-binding displacement assay (n=1)

Ortho and *para*-substituted analogues were deprioritized as they possessed weaker DYRK1A binding affinity. The *N*-methylated matched pairs of **6a**, **8a** and **10a** were synthesised and assayed for DYRK1A binding affinity (Table 3).

Table 3. DYRK1A Binding Affinity of *N*-methylated Pyrazolo[1,5-*b*]pyridazines

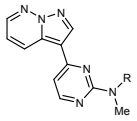

Compound	R	DYRK1A[a]
6b		186
8b		76
10b		97

[a]16-point IC_{50} (nM) in TR-FRET-based ligand-binding displacement assay (n=1)

Despite a reduction in DYRK1A binding affinity by more than 5 fold for all *N*-methylated MMPs, the incorporation of an *N*-methyl group was tolerated surprisingly well in DYRK1A. **8b** and **10b** both maintained high levels of DYRK1A binding affinity (IC_{50} < 100 nM). The binding affinities of MMPs **8a** and **8b** were confirmed by surface plasmon resonance (SPR) measurements, which gave a K_D ± SEM values of 52 ± 4.5 nM for **8b** and 8.9 ± 2.1 nM for **8a** (both n = 2), in good agreement with the binding displacement assay (sensograms are available in supplementary information Figure SI-3).

The broader kinome selectivity of **8b** was determined by the KINOMEscan assay panel (DiscoverX). Percentage inhibition data for CMGC kinases regularly inhibited by DYRK1A inhibitors reported in the literature are summarised in Table 4 (the full dataset is available in the supplementary information).

Table 4. KINOMEscan Selectivity Profiling of **8b**

Kinase	Compound 8b
DYRK1A	65
DYRK1B	0
DYRK2	19
CLK1	59
CLK2	59
CLK3	6
CDK2	12
GSK3β	4
S Score (40)	0.01

[a] % inhibition at 1 μM inhibitor concentration determined in competition binding assay (DiscoverX, n=1).

8b exhibited good kinome-wide selectivity, with a Selectivity Score (S-Score (40)) of 0.01. The successful removal of CDK2 and GSK3β activity with the addition of the *N*-methyl group was consistent with previous results and selectivity against DYRK1B, DYRK2 and CLK3 was also observed. The intrinsic solubility of **8b** was determined by the 'shaking flask' method

in PBS buffer at pH 6.8.[35] **8b** was also profiled for metabolic stability (HLM, RLM). These results are displayed in Table 5.

Table 5: Metabolic Stability and Solubility of **8b**

Compound	HLM	RLM	Solubility
8b	75.0 ± 3.1	805.3 ± 21.6	0.01

HLM and RLM (μL/min/mg) determinations mean of n = 2. HLM = human liver microsomes; RLM = rat liver microsomes; thermodynamic solubility data (mg/mL) derived from single experiment at pH 6.8.

8b exhibited a high rate of metabolic turnover in rat liver microsomes, which would need to be taken into consideration for rodent *in vivo* studies. The solubility of **8b** was not optimal, but was comparable to other DYRK1A tool compounds currently in use. Given the favourable selectivity profile and strong binding affinity for DYRK1A, **8b** was profiled in a MDCK-MDR1 assay to assess whether there were any P-gp or permeability issues with the series.

Table 6. MDCK-MDR1 Permeability of **8b**

Compound	CNS MPO[a] score	Direction = A2B Mean P_{app} (10^{-6} cms^{-1})[b]	Direction = B2A Mean P_{app} (10^{-6} cms^{-1})[b]	Efflux Ratio (Mean P_{app} B2A / Mean P_{app} A2B)[b]
8b	4.8	20.9 ± 0.10	20.1 ± 0.90	0.96

[a]CNS MPO score calculated using CNS MPO KNIME® workflow with ChemAxon nodes. [b]Data generated by Cyprotex in MDCK-MDR1 assay. Permeability coefficient (P_{app}) calculated across cells in direction: A2B (Apical to Basolateral) and B2A (Basolateral to Apical). Determinations ± standard deviation (mean of n =2).

The high CNS MPO score[36] calculated for **8b** correlated with good levels of permeability and low P-gp efflux, indicating that **8b**, and analogues derived from the pyrazolo[1,5-*b*]pyridazine series, stand a good chance of delivering compounds capable of penetrating the blood-brain-barrier (BBB) and exerting an on-target effect *in vivo*.

The co-crystal structure of **6b** bound to DYRK1A (PDB 6S1I) shows that despite possessing an *N*-methyl group close to the hinge of DYRK1A, **6b** is able to adopt a Type I binding mode (Figure 4).

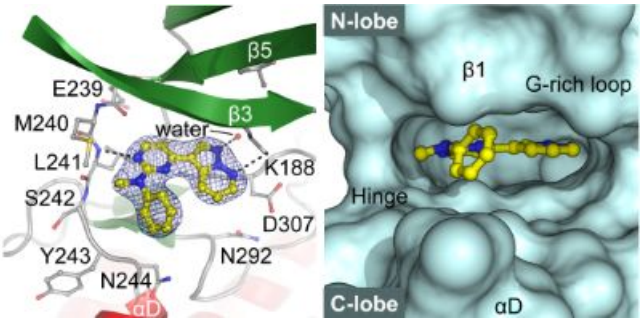

Figure 4. Co-crystal structure of **6b** bound to DYRK1A in Type I fashion, with *N*-methyl group orientated towards the hinge of DYRK1A and Hydrogen-bonding interactions are depicted between the ligand and DYRK1A.

6b bound in a monodentate fashion to the hinge of DYRK1A. The pyridine-type nitrogen of the pyrazolo portion of the pyrazolo[1,5-*b*]pyridazine motif supports a long-range water network at the back of the kinase pocket. The non-bridging nitrogen belonging to the pyridazine portion of the pyrazolo[1,5-*b*]pyridazine motif serves as a hydrogen-bond acceptor (HBA) to the catalytic lysine (Lys188), further stabilizing **6b** in the ATP-site. The hinge-binding motif, bearing an *N*-methyl substituent appears to occupy a small lipophilic pocket present at the hinge of DYRK1A.

6b and **8b** differ only by the addition of a *meta*-methyl group to the phenyl moiety in **8b**, and therefore the crystal structure with **6b** serves as a good model for the binding of **8b**. The lack of literature precedent for the hinge-binding motif and the high-degree of kinome selectivity exhibited by **8b** (S-Score (40) = 0.01), suggests that this pocket may not be present in the vast majority of other kinases. Targeting this pocket appears to be a valid approach to gaining selectivity for DYRK1A.

Conclusion

While structure-based drug design (SBDD) is a proven method for designing selective inhibitors, it remains the case that often, chemical modifications that yield selectivity are found serendipitously and the rationale for compound selectivity can remain unknown. Profiling data already in the public domain can serve as a repository for chemical transformations that can lead to improved selectivity. Data mining tools such as KNIME® can be utilized to extract this information from open-source databases. The method presented here can enable the design of kinase inhibitors with improved selectivity versus off-targets. This strategy serves as a complimentary method to SBDD, helping to rationalize compound selectivity.

The example of DYRK1A, presented here, shows that a chemical modification, which may have been overlooked if ligand data was not already available, can lead to more selectivity against off-targets. A scaffold which was originally developed as a CDK2/4 / GSK3β inhibitor has been repurposed into a selective DYRK1A inhibitor using a chemoinformatics approach. Favourable selectivity against DYRK1B and CLK3 has also been achieved in an efficient manner. This novel class of DYRK1A inhibitors can serve as a basis for future design of CNS-penetrant *in vivo* optimized molecules.

ASSOCIATED CONTENT

Supporting Information

The Supporting Information is available free of charge on the ACS Publications website.

Synthetic chemistry, characterization of compounds, KNIME® workflow, compound SMILES, protein expression, purification, crystallisation, data collection and structure determination (.PDF)

DisoverX KINOMEscan of **8b** (.xlsx)

AUTHOR INFORMATION

Corresponding Author

* Scott H. Henderson; Sussex Drug Discovery Centre, University of Sussex, Brighton, BN1 9RH, U.K.
* Simon E. Ward; Medicines Discovery Institute, Cardiff University, CF10 3AT, U.K. Email: WardS10@cardiff.ac.uk

Present Addresses

† Scott H. Henderson. Warren Center for Neuroscience Drug Discovery, Vanderbilt University, Cool Springs, Tennessee, 37067, United States. Email: scott.h.henderson@vanderbilt.edu

Author Contributions

S.H.H. was involved in the conception and design, acquisition of data, analysis and interpretation of data, and drafting and revising of the article. F.J.S. was involved in the conception and design, acquisition of data, analysis and interpretation of data, and drafting and revising of the article. J.M.B. was involved in the conception and design, acquisition of data, analysis and interpretation of data. M.T.H was involved in the acquisition of data. S.R. was involved in the acquisition of data. I.H.N was involved in the acquisition of data. J.M.E. was involved in the conception of the project, analysis of data and revising of the article. S.E.W. was involved in the conception of the project and revising of the article. All authors approved the final version to be published.

Funding Sources

S.H.H. is funded by the BBSRC (BB/L017105/1); S.E.W. is funded by the Wellcome Trust, MRC, BBSRC and the European Structural Funding via Sêr Cymru scheme. The SGC is a registered charity (number 1097737) that receives funds from AbbVie, Bayer Pharma AG, Boehringer Ingelheim, Canada Foundation for Innovation, Eshelman Institute for Innovation, Genome Canada, Innovative Medicines Initiative (EU/EFPIA) [ULTRA-DD grant no. 115766], Janssen, Merck KGaA Darmstadt Germany, MSD, Novartis Pharma AG, Ontario Ministry of Economic Development and Innovation, Pfizer, São Paulo Research Foundation-FAPESP, Takeda, and Wellcome [106169/ZZ14/Z].

ACKNOWLEDGMENTS

We thank Kamal R. Abdul Azeez and Ana Clara Redondo for help with protein purification. An academic license for ChemAxon (https://www.chemaxon.com) and a license for ChemAxon Infocom KNIME nodes is gratefully acknowledged. We would also like to acknowledge the platform KNIME® (https://www.knime.com) and the ChEMBL group at EMBL-EBI for donating the NN-Activity Pairs KNIME workflow to the KNIME community.

ABBREVIATIONS

BBB: blood-brain barrier; CDK: cyclin dependent kinase; CLK: CDC-like kinases; CMGC: Including cyclin-dependent kinases (CDKs), mitogen-activated protein kinases (MAP kinases), glycogen synthase kinases (GSK) and CDK-like kinases; CNS MPO: Central nervous system multi-parameter optimization; DYRK: Dual-specificity tyrosine phosphorylation-regulated kinase; GSK: Glycogen synthase kinases; HBA: hydrogen bond acceptor; HLM: human liver microsomes; MDCK-MDR1: Madin-Darby canine kidney cells transfected with the human MDR1 gene; MMP: matched-molecular pair; PBS: Phosphate-buffered saline; PDB: Protein databank; PKIS: published kinase inhibitor set; RLM: rat liver microsomes; SBDD: structure-based drug design.

REFERENCES

[1] Wu, P.; Nielsen, T. E.; Clausen, M. H. Small-molecule kinase inhibitors: an analysis of FDA-approved drugs. Drug Discov. Today. **2016**. *21*(1), 5-10.

[2] Davis, M. I.; Hunt, J. P.; Herrgard, S.; Ciceri, P.; Wodicka, L. M.; Pallares, G.; Hocker, M.; Treiber, D. K.; Zarrinkar, P. P. Comprehensive analysis of kinase inhibitor selectivity. Nat. Biotechnol. **2011**. *29*, 1046-1051.

[3] Zhao, Z.; Xie, L.; Bourne, P. E. Insights into the binding mode of MEK type-III inhibitors. A step towards discovering and designing allosteric kinase inhibitors across the human kinome. PLoS One. **2017**. *12*(6): e0179936.

[4] Roskoski, Jr. R. Classification of small molecule protein kinase inhibitors based upon the structures of their drug-enzyme complexes. Pharmacological Research. **2016**. *103*, 26–48.

[5] Anastassiadis, T.; Deacon, S. W.; Devarajan, K.; Ma, H.; Peterson, J. R. Comprehensive assay of kinase catalytic activity reveals features of kinase inhibitor selectivity. Nat. Biotechnol. **2011**. *29*, 1039–1045.

[6] Metz, J. T.; Johnson, E. F.; Soni, N. B.; Merta, P. J.; Kifle, L.; Hajduk, P. J. Navigating the kinome. Nat. Chem. Biol. **2011**. *7*(4), 200-202.

[7] Elkins, J. M.; Fedele, V.; Szklarz, M.; Abdul Azeez, K. R.; Salah, E.; Mikolajczyk, J, Romanov, S.; Sepetov, N.; Huang, X. P.; Roth, B. L.; Al Haj Zen, A.; Fourches, D.; Muratov, E.; Tropsha, A.; Morris, J.; Teicher, B. A.; Kunkel, M.; Polley, E.; Lackey, K. E.; Atkinson, F. L.; Overington, J. P.; Bamborough, P.; Müller, S.; Price, D. J.; Willson, T. M.; Drewry, D. H.; Knapp, S.; Zuercher, W. J. Comprehensive characterization of the Published Kinase Inhibitor Set. Nat. Biotechnol. **2016**. *34*(1), 95–103.

[8] Drewry, D. H.; Willson, T. M.; Zuercher, W. J. Seeding collaborations to advance kinase science with the GSK Published Kinase Inhibitor Set (PKIS). Curr. Top. Med. Chem. **2014**. *14*(3), 340–342.

[9] Drewry, D. H.; Wells, C. I.; Andrews, D. M.; Angell, R.; Al-Ali, H.; Axtman, A. D.; Capuzzi, S. J.; Elkins, J. M.; Ettmayer, P.; Frederiksen, M.; Gileadi, O.; Gray, N.; Hooper, A.; Knapp, S.; Laufer, S.; Luecking, U.; Michaelides, M.; Müller, S.; Muratov, E.; Denny, R. A.; Saikatendu, K. S.; Treiber, D. K.; Zuercher, W. J.; Willson, T. M. Progress towards a public chemogenomic set for protein kinases and a call for contributions. PLoS One. **2017**. *12*(8), e0181585.

[10] Bento, A. P.; Gaulton, A.; Hersey, A.; Bellis, L. J.; Chambers, J.; Davies, M.; Krüger, F. A.; Light, Y.; Mak, L.; McGlinchey, S.; Nowotka, M.; Papadatos, G.; Santos, R.; Overington, J. P. The ChEMBL bioactivity database: an update. Nucleic Acids Res. **2014**. *42*, 1083-1090.

[11] Berthold, M. R.; Cebron, N.; Dill, F.; Gabriel, T. R.; Kötter, T.; Meinl, T.; Ohl, P.; Thiel, K.; Wiswedel, B. KNIME - the Konstanz information miner: version 2.0 and beyond. ACM SIGKDD Explor Newslett. **2009**. *11*, 26–31.

[12] Pathak, A.; Rohilla, A.; Gupta, T.; Akhtar, M. J.; Haider, M. R.; Sharma, K.; Haider, K.; Yar, M. S. DYRK1A kinase inhibition with emphasis on neurodegeneration: A comprehensive evolution story-cum-perspective. Eur. J. Med. Chem. **2018**. *158*, 559-592.

[13] Smith, B.; Medda, F.; Gokhale, V.; Dunckley, T.; Hulme, C. Recent advances in the design, synthesis, and biological evaluation of selective DYRK1A inhibitors: a new avenue for a disease modifying treatment of Alzheimer's? ACS Chem. Neurosci. **2012**, 3, 857-872.

[14] Ferrer, I.; Barrachina, M.; Puig, B.; Martinez de Lagran, M.; Marti, E.; Avila, J.; Dierssen, M. Constitutive Dyrk1A is abnormally expressed in Alzheimer disease, Down syndrome, Pick disease, and related transgenic models. Neurobiol. Dis. **2005**. *20*, 392-400.

[15] Nguyen, T. L.; Fruit, C.; Hérault, Y.; Meijer, L.; Besson, T. Dual-specificity tyrosine phosphorylation-regulated kinase 1A (DYRK1A) inhibitors: a survey of recent patent literature. Expert Opin. Ther. Pat. **2017**. *27*(11), 1183-1199.

[16] Wegiel, J.; Gong, C. X.; Hwang, Y. W. The role of DYRK1A in neurodegenerative diseases. FEBS J. **2011**. *278*(2), 236-45.

[17] Duchon, A.; Herault, Y. DYRK1A, a Dosage-Sensitive Gene Involved in Neurodevelopmental Disorders, Is a Target for Drug Development in Down Syndrome. Front. Behav. Neurosci. **2016**. *10*, 104.

[18] Schnabel, F.; Smogavec, M.; Funke, R.; Pauli, S.; Burfeind, P.; Bartels, I. Down syndrome phenotype in a boy with a mosaic microduplication of chromosome 21q22. Mol. Cytogenet. **2018**. *11*, 62.

[19] Ryoo, S. R.; Jeong, H. K.; Radnaabazar, C.; Yoo, J. J.; Cho, H. J.; Lee, H. W.; Kim, I. S.; Cheon, Y. H.; Ahn, Y. S.; Chung, S. H.; Song, W. J. DYRK1A-mediated hyperphosphorylation of Tau. A functional link between Down syndrome and Alzheimer disease. J. Biol. Chem. **2007**. *282*(48), 34850-34857.

[20] Kimura, R.; Kamino, K.; Yamamoto, M.; Nuripa, A.; Kida, T.; Kazui, H.; Hashimoto, R.; Tanaka, T.; Kudo, T.; Yamagata, H.; Tabara, Y.; Miki, T.; Akatsu, H.; Kosaka, K.; Funakoshi, E.; Nishitomi, K.; Sakaguchi, G.; Kato, A.; Hattori, H.; Uema, T.; Takeda, M. The DYRK1A gene, encoded in chromosome 21 Down syndrome critical region, bridges between beta-amyloid

production and tau phosphorylation in Alzheimer disease. Hum. Mol. Genet. **2007**. *16*(1), 15-23.
[21] Lautarescu, B. A.; Holland, A. J.; Zaman, S. H. The Early Presentation of Dementia in People with Down Syndrome: a Systematic Review of Longitudinal Studies. Neuropsychol. Rev. **2017**. *27*(1), 31-45.
[22] Becker, W.; Joost, H. G. Structural and functional characteristics of Dyrk, a novel subfamily of protein kinases with dual specificity. Prog. Nucleic Acid Res. Mol. Biol. **1999**. *62*, 1-17.
[23] Becker, W.; Sippl, W. Activation, regulation, and inhibition of DYRK1A. FEBS J. **2011**. *278*, 246-256.
[24] Aranda, S.; Laguna, A.; de la Luna, S. DYRK family of protein kinases: evolutionary relationships, biochemical properties, and functional roles. FASEB J. **2011**. *25*, 449-462.
[25] Soundararajan, M.; Roos, A. K.; Savitsky, P.; Filippakopoulos, P.; Kettenbach, A. N.; Olsen, J. V.; Gerber, S. A.; Eswaran, J.; Knapp, S.; Elkins, J. M. Structures of Down syndrome kinases, DYRKs, reveal mechanisms of kinase activation and substrate recognition. Structure. **2013**. *21*(6), 986–996.
[26] Jarhad, D. B.; Mashelkar, K. K.; Kim, H-R.; Noh, M.; Jeong, L. S. Dual-Specificity Tyrosine Phosphorylation-Regulated Kinase 1A (DYRK1A) Inhibitors as Potential Therapeutics. J. Med. Chem. **2018**. *61*(22), 9791-9810.
[27] Park, J.; Song, W.J., Chung, K.C. Function and regulation of Dyrk1A: towards understanding Down syndrome. Cell. Mol. Life Sci. **2009**. *66*, 3235-3240.
[28] Workman, P.; Collins, I. Probing the probes: fitness factors for small molecule tools. Chem. Biol. **2010**, *17*(6), 561-577.
[29] Tahtou, T.; Elkins, M. J.; Filippakopoulos, P.; Soundararajan, M.; Burgy, G.; Durieu, E.; Cochet, C.; Schmid, R. S.; Lo, D. C.; Delhommel, F.; Oberholzer, A. E.; Pearl, L. H.; Carreaux, F.; Bazureau, J-P.; Knapp, S.; Meijer, L. Selectivity, cocrystal structures, and neuroprotective properties of leucettines, a family of protein kinase inhibitors derived from the marine sponge alkaloid leucettamine B. J. Med. Chem. **2012**. *55*, 9312-9330.
[30] Foucourt, A.; Hédou, D.; Dubouilh-Benard, C.; Désiré, L.; Casagrande, A. S.; Leblond, B.; Loäec, N.; Meijer, L.; Besson, T. Design and synthesis of thiazolo[5,4-f]quinazolines as DYRK1A inhibitors, part II. Molecules. **2014**, *19*, 15411-15439.
[31] Woods, Y. L.; Cohen, P.; Becker, W.; Jakes, R.; Goedert, M.; Wang, X.; Proud, C.G. The kinase DYRK phosphorylates protein-synthesis initiation factor eIF2Bepsilon at Ser539 and the microtubule-associated protein tau at Thr212: potential role for DYRK as a glycogen synthase kinase 3-priming kinase. Biochem. J. **2001**. 355, 609–615.
[32] Neagoie, C.; Vedrenne, E.; Buron, F.; Mérour, J. Y.; Rosca, S.; Bourg, S.; Lozach, O.; Meijer, L.; Baldeyrou, B.; Lansiaux, A.; Routier, S. Synthesis of chromeno[3,4-*b*]indoles as Lamellarin D analogues: a novel DYRK1A inhibitor class. Eur. J. Med. Chem. **2012**. *49*, 379-396.
[33] Tavares, F. X.; Boucheron, J. A.; Dickerson, S. H.; Griffin, R. J.; Preugschat, F.; Thomson, S. A.; Wang, T. Y.; Zhou, H. Q. *N*-Phenyl-4-pyrazolo[1,5-*b*]pyridazin-3-ylpyrimidin-2-amines as potent and selective inhibitors of glycogen synthase kinase 3 with good cellular efficacy. J. Med. Chem. **2004**. *47*(19), 4716-4730.
[34] Stevens, K. L.; Reno, M. J.; Alberti, J. B.; Price, D. J.; Kane-Carson, L. S.; Knick, V. B.; Shewchuk, L. M.; Hassell, A. M.; Veal, J. M.; Davis, S. T.; Griffin, R. J.; Peel, M. R. Synthesis and evaluation of pyrazolo[1,5-*b*]pyridazines as selective cyclin dependent kinase inhibitors. Bioorg. Med. Chem. Lett. **2008**. *18*(21), 5758-5762.
[35] Lipinski, C. A.; Lombardo, F.; Dominy, B. W.; Feeney, P. J. Experimental and computational approaches to estimate solubility and permeability in drug discovery and development settings. Adv. Drug Deliv. Rev. **1997**. *23*, 3–25.
[36] Wager, T. T.; Hou, X.; Verhoest, P. R.; Villalobos, A. Moving beyond rules: the development of a central nervous system multiparameter optimization (CNS MPO) approach to enable alignment of druglike properties. ACS Chem. Neurosci. **2010**. *1*(6), 435-449.